



A multiscale approach for the seismic analysis of concrete gravity dams



Marco Paggi^{a,*}, Giuseppe Ferro^a, Franco Braga^b

^a Politecnico di Torino, Department of Structural, Geotechnical and Building Engineering, C.so Duca degli Abruzzi 24, 10129 Torino, Italy

^b Università di Roma La Sapienza, Department of Structural and Geotechnical Engineering, Via Eudossiana 18, 00198 Roma, Italy

ARTICLE INFO

Article history:

Received 4 June 2012

Accepted 11 March 2013

Available online 11 April 2013

Keywords:

Interface crack propagation
Nonlinear fracture mechanics
Concrete dams
Seismic loading
Size-scale effects

ABSTRACT

In this article, the problem of cracking in concrete gravity dams subjected to seismic loadings is examined under a multiscale perspective. Preliminarily, the size-scale effects on the mechanical parameters entering the nonlinear constitutive models of the interface crack are discussed. From a wide review of existing experimental results, it is shown that the material tensile strength, the fracture energy, the friction coefficient and the concrete compressive strength are strongly size-scale dependent. This evidence pinpoints the necessity of performing experimental testing on large scale specimens to assess the value of the parameters to be used in nonlinear fracture mechanics simulations. Moreover, the size-scale dependency of the interface constitutive properties implies the necessity of updating their values during crack propagation simulations. To do so, interface properties are not given in input a priori, but they are selected at each step of the simulation according to the specified scaling laws. The numerical simulations, based on the finite element method and a generalized interface constitutive law for contact and decohesion implemented in the node-to-segment contact strategy, show the high sensitivity of the phenomenon of crack propagation by the parameters of the damage law used to degrade the cohesive zone properties in case of repeated cycles.

© 2013 Elsevier Ltd. All rights reserved.

1. Introduction

Structural integrity assessment of concrete gravity dams has long been investigated. The first attempts to apply the theories and the methods of fracture mechanics to concrete structures are dated back to the 1970s [1]. Pioneering analyses were mostly based on linear elastic fracture mechanics (LEFM). Crack growth takes place when an equivalent stress-intensity factor, accounting for Mixed-Mode loading, reaches the critical stress-intensity factor, which is a material property that defines the toughness of concrete. This approach is suitable when the size of the process zone is small as compared to the structural size, a condition usually satisfied in large scale structures like dams.

The first systematic application of fracture mechanics to dams was proposed in the 15th International Congress on Large Dams, ICOLD, held in Lausanne in 1985 (see, for instance, the guidelines proposed by Linsbauer [2] for the application of LEFM to dams). The problem of cracking in concrete dams was perceived as a problem of paramount importance, both for the existing structures, and for the design of the new ones. Hence, it was ascertained that the phenomenon of cracking cannot be totally avoided during the realization stage and in the service conditions [3]. The main reasons are the temperature excursions between the internal and the

external sides of the dam, dilatation of concrete when exposed to environmental conditions, as well as foundation settlements. LEFM theories were then applied to several case studies, including the analysis of cracking in the Fontana dam in North Carolina (USA) [4,5], in the Koyna dam in India [6–8], and in the Köhlbrein dam in Austria [9–11]. Recently, LEFM has also been applied to the interpretation of the reasons for collapse of the Malpasset dam in France [12].

Experimental tests on scaled down models have been performed in the past [13] to assess the reliability of LEFM predictions. On the other hand, seismic fracture analyses are quite scarce due to their high complexity [6,7,14]. Cracks encountered in dams require special modeling when subjected to crack closure, as it happens during repeated loadings [7]. When nonlinear fracture mechanics (NLFM) models are used [14,15], a nonlinear dynamic problem has to be solved [14], which is nowadays challenging due to the large differences in the characteristic time scales of the problem.

In the present paper, the phenomenon of crack propagation at the interface between the concrete dam and the rock foundation is investigated. This source of damage is particularly important from the structural integrity point of view. In fact, besides Mixed-Mode crack growth in concrete, dam failure is often the result of crack propagation along the rock–concrete interface at the dam foundation. In this case, there is a lack of predictive models in the literature, especially for seismic analyses. A preliminary study on the possibility to use nonlinear fracture mechanics cou-

* Corresponding author. Tel.: +39 0110904910; fax: +39 0110904899.

E-mail address: marco.paggi@polito.it (M. Paggi).

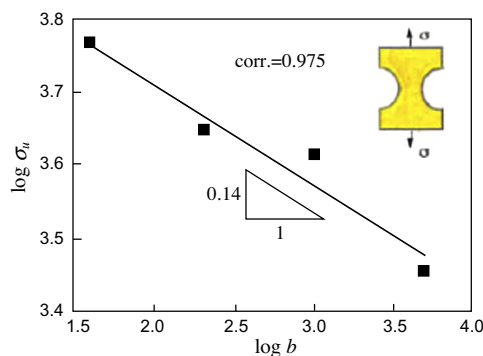
pled with damage mechanics and contact mechanics in dynamics has been outlined in [16].

In the present work, the problem of size-scale effects on the tensile strength, fracture energy and dissipated energy in compression is critically analyzed. It is found that huge structures like dams are very sensible to size-scale effects and suitable parameters have to be used in the NLFM models for the simulation of crack propagation. From the numerical point of view, an adaptive approach is used, where the material parameters are selected at each step of the simulation according to the given scaling laws. Then, the generalized interface constitutive law proposed in [17] is used to model the phenomenon of crack closing and reopening at the interface and its finite element implementation in the code FEAP is discussed. In particular, following [16], a damage variable is introduced in the cohesive zone formulation in order to predict crack propagation under repeated loadings, in close similarity with the phenomenon of fatigue crack growth. Finally, a case study is reported in the paper showing the capabilities of the proposed approach and the sensitivity to the parameters of the damage law.

2. Size-scale effects on the mechanical parameters

The numerical simulation of the behavior of dams subjected to cracking requires the knowledge of the mechanical properties of concrete and cold interfaces, to be used as input of the constitutive models. For concrete, the tensile and compressive strengths and the fracture energy are the most important parameters. The use of concrete with large sized aggregates leads to severe size effects and the applicability of standard testing procedures at the laboratory scale to determine mechanical parameters is rather questionable [18]. In this context, the wide experimental campaign carried out by Carpinteri and Ferro [19,20] in the Laboratory of Structural Mechanics of Politecnico di Torino on concrete specimens with different sizes has shown that the tensile strength of concrete, σ_u , is a decreasing function of the structural size, b . In particular, an approximate scaling law with negative exponent equal to -0.14 was found, see Fig. 1(a). An opposite trend was observed for the fracture energy [21], as illustrated in Fig. 1(b), where the scaling is well approximated by a power-law with positive exponent equal to 0.38.

Size-scale effects on the compressive behavior of quasi-brittle materials are also observed. For instance, size-scale effects on the dissipated energy in compression have been reported in [22] by considering a scale range 1:19 between the smallest and the biggest specimen. The tested cylinder specimens had a height–diameter ratio, b/d , equal to 1. The stress–strain curves corresponding to 4 different specimens (C13 corresponds to $b = 10$ mm; C21 to $b = 23$ mm; C33 to $b = 46$ mm; C44 to $b = 100$ mm) are shown in



(a) Scaling law for the tensile strength.

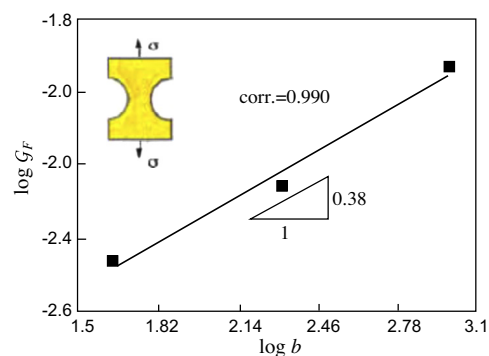
Fig. 2(a). The area under such curves defines the energy density S dissipated in compression. This quantity is a decreasing function of the specimen size according to a power-law with negative exponent, see Fig. 2(b).

For concrete–concrete and rock–concrete interfaces, on the other hand, we need to know their peak stress σ_{max} and their fracture energy G_{int} for the characterization of the cohesive zone model. Moreover, the evolution of damage in case of repeated loading should also be quantified in order to perform a full characterization. In case of crack propagation, the frictional response has also to be quantified. However, experimental studies are quite scarce in the literature. Kishen and Rao [23] have pointed out that the fracture energy of the interface decreases as the difference in the compressive strengths of the materials sharing the interface increases. This implies that the fracture energy of a patch-repaired concrete should not be very much different from that of the parent concrete in patch repair systems. The same should apply when the compressive strength of rock is similar to that of concrete. Moreover, in case of interface specimens, the strength was found to be a decreasing function of the specimen size, in analogy with that observed in pure concrete.

Regarding the frictional response, size-scale effects are expected in case of rock–rock frictional contact due to roughness [24]. Bandis et al. [25] observed that the peak shear stress before sliding increases by reducing the size of the tested specimens. They cast 360–400 mm long replicas of eleven natural joint surfaces with a wide range of different roughnesses, using artificial rock material. For each of the natural joint surfaces considered, several specimens were prepared which, for practical purposes, could be considered identical. For each natural joint, a full size replica was subjected to direct shear testing under constant compressive stress. Then, another replica of the same joint was sawn into four parts with each part being subjected to shear testing under the same nominal compressive stress. On the remaining samples, further subdivisions were created and tested. Shear stress vs. shear displacement results are shown in Fig. 3, in which the size-scale effect on the peak shear stress is clearly evidenced. Dividing the peak shear stress in the curves in Fig. 3 by the applied nominal pressure, size-scale effects on the friction coefficient can be put into evidence, see Fig. 4.

3. Interface constitutive model

A general constitutive model is proposed in this section, as a result of the combination of a cohesive zone model (to depict fracture), a contact model (to model contact in case of load reversal and in case of unbonded interfaces) and a damage model (to capture finite life effects in case of repeated loading).



(b) Scaling law for the fracture energy.

Fig. 1. Scaling laws for tensile strength and fracture energy of concrete [19–21].

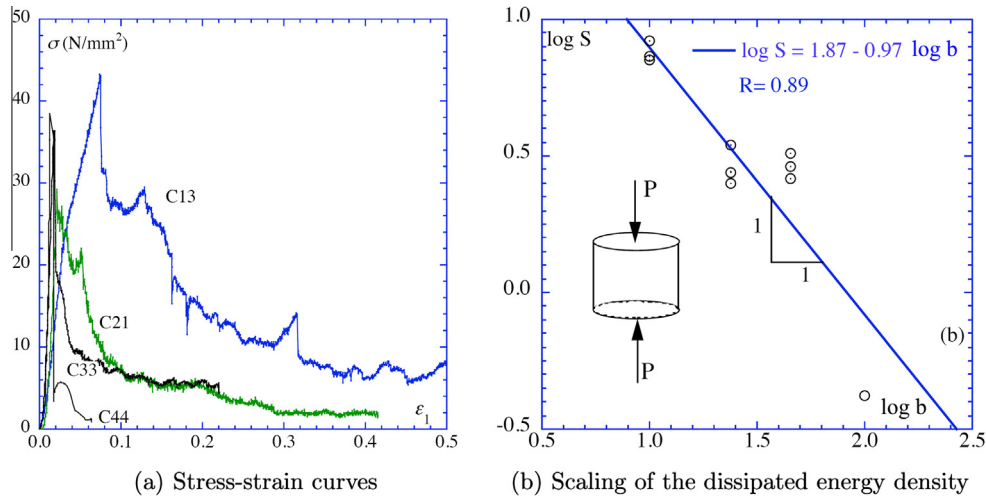


Fig. 2. (a) Stress–strain curves of compressed specimens with different size (C13: $b = 10$ mm; C21: $b = 23$ mm; C33: $b = 46$ mm; C44: $b = 100$ mm). (b) Scaling of the dissipated energy density, S , with the sample size, b . Data obtained from [22].

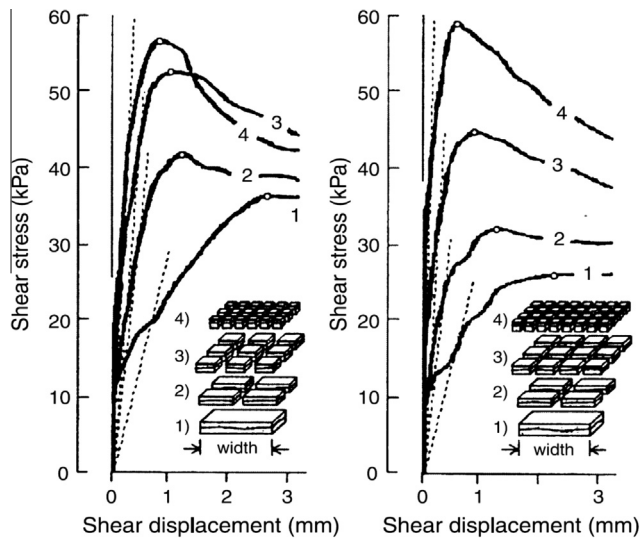


Fig. 3. Experimental results of shear tests on rock joints [25].

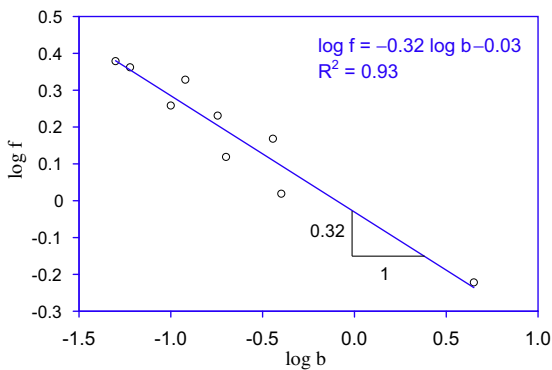


Fig. 4. Size-scale effects on the friction coefficient (data from Fig. 3).

3.1. Cohesive zone model

Interface fracture between concrete and rock is herein modeled in the framework of NLFM, using the interface cohesive zone model proposed by Geubelle and Baylor [26]. This model, originally ap-

plied to composite materials, represents a natural extension of the classical bilinear cohesive zone models to Mixed-Mode interface crack problems, where Mode Mixity is usually an important issue that cannot be disregarded. Following this approach, a measure of interface opening and sliding, λ , is introduced:

$$\lambda = \sqrt{\left(\frac{g_N}{l_{Nc}}\right)^2 + \left(\frac{g_T}{l_{Tc}}\right)^2}, \tag{1}$$

where g_N and g_T denote, respectively, the normal and the tangential separations. Parameters l_{Nc} and l_{Tc} are the critical values for the normal and the tangential gaps. They correspond to the separation for which cohesive forces transmitted through the interface vanish, i.e., complete debonding takes place. Normal and tangential cohesive tractions are given as functions of interface opening in the process zone:

$$F_N = \begin{cases} \frac{\sigma_{max}}{\lambda_{max}} \frac{g_N}{l_{Nc}} & 0 < \lambda \leq \lambda_{max}, \\ \frac{\sigma_{max}}{\lambda} \frac{1-\lambda}{1-\lambda_{max}} \frac{g_N}{l_{Nc}} & \lambda_{max} < \lambda < 1; \end{cases} \tag{2}$$

$$F_T = \begin{cases} \frac{\tau_{max}}{\lambda_{max}} \frac{l_{Nc}}{l_{Tc}} \frac{g_T}{l_{Tc}} & 0 < \lambda \leq \lambda_{max}, \\ \frac{\tau_{max}}{\lambda} \frac{1-\lambda}{1-\lambda_{max}} \frac{l_{Nc}}{l_{Tc}} \frac{g_T}{l_{Tc}} & \lambda_{max} < \lambda < 1. \end{cases} \tag{3}$$

The effect of coupling between normal and tangential displacements upon normal and tangential tractions is shown in Fig. 5 for $\lambda_{max} = 0.2$. For either pure normal separation (Mode I), i.e. for $g_T = 0$, or for pure tangential separation (Mode II), i.e. for $g_N = 0$, the classical bilinear cohesive laws are obtained as limit cases.

The limit situation of a pure Mode II deformation deserves particular attention. The shear response of rough interfaces, as in case of cold joints, is very complex. Examining the shear test results in Fig. 3, we note that the shear stress is a nonlinear increasing function of the sliding displacement up to a peak value. This is the result of the progressive stick–slip transition of multiple asperities in contact subjected to a non-uniform normal pressure at the micro-scale. After reaching a peak shear stress, a softening branch is observed. In this second stage, the interface behavior is ruled by interlocking between asperities and their progressive shearing. In the present work, this complex nonlinear response in Mode II governed by contact mechanics at the microscale has been simplified by adopting a bilinear cohesive zone model with softening (see Fig. 5, $l_{Tc}/l_{Nc} = 1$). In this limit case of pure Mode II deformation, the computation switches to a contact formulation with a constant

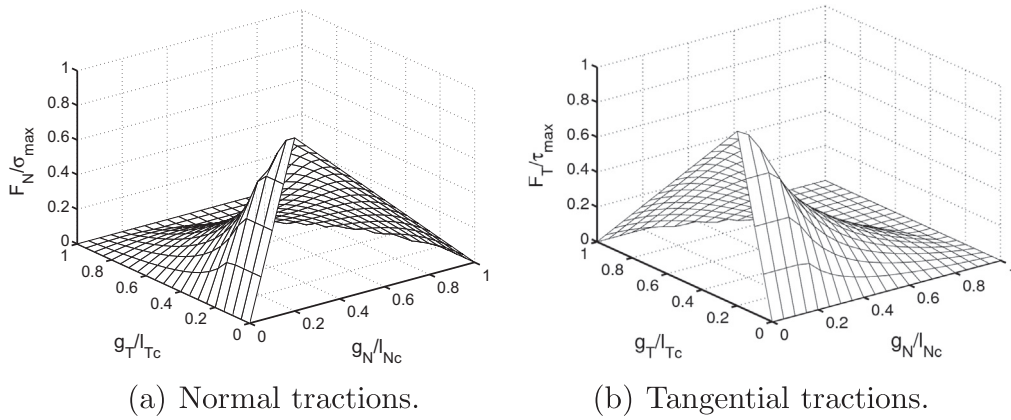


Fig. 5. Normal and tangential tractions vs. normal and tangential separations for $\lambda_{max} = 0.2$ and $l_{Tc}/l_{Nc} = 1$.

(residual) friction coefficient when interface decohesion takes place, see Section 3.2.

Crack propagation in quasi-brittle materials can be numerically modeled by using either extrinsic or intrinsic cohesive zone models. For extrinsic models, cohesive elements are adaptively inserted into the mesh. This usually requires complicated updating schemes for the modified mesh by renumbering nodes and elements. Moreover, they assume that separation only occurs when the interfacial traction reaches the tensile strength of the material and, once this condition is achieved, the interfacial traction monotonically decreases as separation increases. In this scheme, there is no initial compliance in the CZM, i.e., $\lambda_{max} = 0$ in Eqs. (2) and (3). Intrinsic models, on the other hand, require that all the interface/contact elements are embedded in the discretized structure from the beginning of simulation. For this reason, intrinsic CZMs assume that, e.g. in pure Mode I, traction increases with increasing interfacial gap up to a maximum and then decreases and finally vanishes at a characteristic separation, where complete decohesion occurs. In this case, $\lambda_{max} \neq 0$ and an artificial compliance is introduced in the FE model. If the crack grows along a pre-defined path, as in the problem addressed herein, this approach is computationally stable and efficient. The choice of λ_{max} has a role on the mechanical response and it is usually kept as small as possible in the numerical simulations to avoid a physically not realistic high interface compliance [27]. Physically, The choice of $\lambda_{max} = 0.2$ implies that the peak cohesive tractions are reached when the opening and sliding relative displacements are equal to 1/5 of their critical values for decohesion or the achievement of the residual shear resistance. In Mode II, this is qualitatively supported by the linearized shear responses in Fig. 3 (dashed lines).

3.2. Contact model

Cohesive models can be used for studying the debonding stage, until a complete interfacial separation occurs. However, due to repeated loadings, a proper modeling of crack closure is also required in order to fully characterize the mechanical behavior of interfaces. This is achieved using the generalized interface constitutive law proposed in [17]. When interface closure takes place, the unilateral contact constraints are imposed, i.e.: (i) penetration is not allowed, i.e. $g_N \geq 0$; (ii) a closed gap between the bodies leads to compressive contact tractions, i.e., if $g_N = 0$, then $F_N < 0$. When the gap is open, tractions are either equal to zero (debonded interface) or are computed according to the cohesive zone model outlined in the previous section.

Therefore, in analogy with the continuum, where it is required the expression of the total potential energy of the mechanical sys-

tem to set up the finite element formulation, the contact problem corresponds to finding the minimum of a functional under boundary conditions expressed in terms of inequalities [28]. In addition to the typical displacement unknowns of the finite element method, the non-compenetrability conditions give rise to another set of unknowns, corresponding to the contact forces, F_N , acting at each finite element node along the interface. In this framework, the numerical techniques for the solution of such problems can be grouped into two main categories: those that satisfy the geometrical non-compenetrability condition exactly, and those that satisfy this condition only in an approximate way.

In this study, the penalty method is adopted, which belongs to the second category. This technique presents the advantage that the number of equations related to the continuum discretization is not increased in the analysis. This permits to deal with a positively defined stiffness matrix with constant dimensions. According to this approach, for a given value of the normal gap, g_N , the corresponding normal force, F_N , is computed as the product of a penalty parameter, C , and the current value of the interpenetration. Clearly, the unilateral constraint condition is recovered only for values of the penalty parameter tending to infinity. In the standard version of this technique, the penalty parameter C is just a constant coefficient, selected high enough to approximate the unilateral contact constraint. From the mechanical point of view, this method corresponds of interposing a bed of linear springs between the contact faces (see the linear curve (c) in Fig. 6). In the present study, a nonlinear variant of this approach is adopted, motivated by roughness of cracks [29]. A non-zero gap g_N can be physically motivated by considering a progressive flattening of the asperities whose heights are randomly distributed with respect to an average mean plane (see Fig. 7). This process leads to a contact stiffness nonlin-

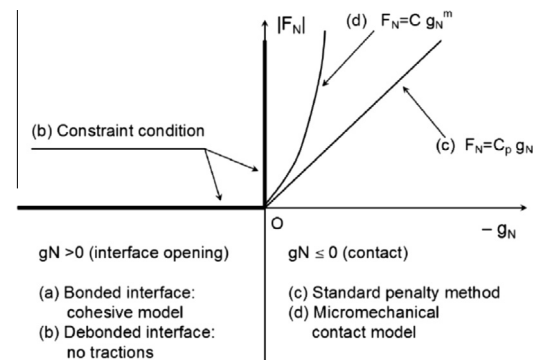


Fig. 6. The role of penalty parameter in contact problems.

early dependent on the normal gap g_N (see the curve (d) in Fig. 6). For the numerical simulations, the micromechanical contact parameters obtained in [29] for fractal surfaces with a fractal dimension $D_f = 2.3$ are selected.

As far as the response of the joint in the tangential direction is concerned, two different situations have to be considered: in the first one, no tangential relative displacement occurs in the contact zone subjected to a tangential force, F_T . This behavior is called stick. The second situation is represented by a relative tangential displacement, g_T , along the contact interface, which is the so-called slip. Stick is equivalent to the case where the relative tangential velocity is zero. Hence, the stick condition can be obtained as [30]:

$$\dot{g}_T = 0. \quad (4)$$

This condition is formulated in the current configuration and thus, in general, it imposes a nonlinear constraint equation on the motion along the contact interface. Sliding takes place when the tangential forces are above a certain limit, and the contacting surfaces move relative to each other. In our model, sliding is described by the Coulomb law:

$$F_T = -f|F_N| \frac{\dot{g}_T}{|\dot{g}_T|}, \quad \text{if } |F_T| > f|F_N|, \quad (5)$$

where the parameter f denotes the friction coefficient.

3.3. Damage model for repeated loadings

In addition to the above traction-separation relations describing the behavior of interfaces under tension/compression, a description of the damage evolution has to be provided in order to capture finite life effects in the case of repeated loading. To this aim, the initial cohesive strengths, σ_{\max} and τ_{\max} are replaced at each step by the actual cohesive strengths, σ_{\max}^t and τ_{\max}^t , which take into account the degradation of the cohesive law:

$$\sigma_{\max}^t = \sigma_{\max}(1 - D), \quad \tau_{\max}^t = \tau_{\max}(1 - D), \quad (6)$$

where D is the damage variable.

To compute the current state of damage, a description of the evolution of damage has to be provided. For cyclic loading, the damage evolution equation has to characterize the failure of the cohesive zone model due to cycling at subcritical loads. As a fundamental hypothesis, we assume that the increment of damage is related to the increment of deformation times a function of the stress level, similarly to the model proposed by Roe and Siegmund [31]:

$$\dot{D} = \left(\frac{\Delta g}{g_{\max}}\right)^\alpha \left(\frac{F}{\sigma_{\max}^t} - \frac{F_{th}}{\sigma_{\max}}\right)^\beta \quad 0 \leq \dot{D} \leq 1, \quad (7)$$

where $g = \sqrt{g_N^2 + g_T^2}$ is the resultant separation at a given time step. Hence, $\Delta g = g^{t+\Delta t} - g^t$ represents the increment of deformation from one time step to the next. The variable g_{\max} denotes the maximum cumulative separation length to achieve failure of the cohesive zone under cyclic loading. Finally, $F = \sqrt{F_N^2 + F_T^2}$ is the resultant traction

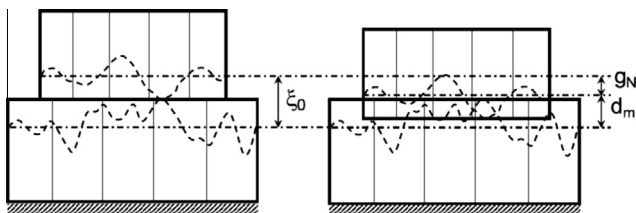


Fig. 7. The meaning of the normal gap g_N in the framework of contact mechanics between rough surfaces. The variable ξ_0 denotes the mean plane separation at first contact, whereas d_m is the actual mean plane separation.

and F_{th} is a threshold value below which no damage occurs. The two exponents α and β are related to the severity of damage.

The applicability of Eq. (7) to fatigue crack growth in concrete has been proven in [32]. In case of a Mode I problem with subcritical repeated loadings, this approach based on damage mechanics was able to accurately predict the plate deformation at the maximum stress level as a function of the number of loading cycles. The agreement with experimental results was notably good.

The damage model used in the present work was motivated by the former application by Roe and Siegmund [31] of CZMs in fatigue. In that work, a single scalar damage variable was used to degrade the cohesive properties as a whole, as in the present study. This assumption implies that repeated sub-critical separations globally affect the CZM response in the same way, regardless of Mode Mixity. The use of two different damage functions could be possible in the present CZM formulation, where the CZM has a bilinear shape not obtained from a single potential function. In other cases where a potential function is used to define the shape of the CZM in Mode Mixity (see [31]), a single damage variable has to be defined. At present, however, no experimental evidence to support the use of two different damage variables has been provided and therefore one single damage variable is used.

It is important to notice that the cumulative separation g_{\max} is computed by adding only positive separation increments Δg , i.e., only during opening and not closing of the interface. In practice, this implies that reloading contributes to damage accumulation, whereas unloading does not. To complete the formulation, the current damage is computed as:

$$D = \int_0^t \dot{D} dt. \quad (8)$$

4. Finite element algorithms

In the finite element formulation, the contributions of the nodal normal and tangential contact and cohesive forces are added to the global virtual work equation [33]:

$$\delta W = Ah(F_N \delta g_N + F_T \delta g_T), \quad (9)$$

where the symbol A denotes an assembly operator for all the interface nodes and h is the size of the finite element. A main difficulty with the analysis, stemming from the contact constraints and the imperfect bonding, is that the extension of the contact and debonded zones are unknown *a priori*, and the corresponding boundary value problem must be solved with an iterative method. The Newton–Raphson solution procedures commonly used for solving nonlinear problems require the determination of the tangent stiffness matrix. Consistent linearization of the equation set (9) leads to:

$$\Delta \delta W = h \left(\frac{\partial F_N}{\partial g_N} \Delta g_N + \frac{\partial F_N}{\partial g_T} \Delta g_T \right) \delta g_N + h \left(\frac{\partial F_T}{\partial g_N} \Delta g_N + \frac{\partial F_T}{\partial g_T} \Delta g_T \right) \delta g_T + h F_N \Delta \delta g_N + h F_T \Delta \delta g_T \quad (10)$$

where the symbol δ has been used for variations and the symbol Δ denotes linearizations. Linearizations and variations of the normal and the tangential gaps can be obtained as in [30], as well as the discretized version of these expressions for a direct implementation in the finite element formulation based on the node-to-segment contact strategy.

Regarding the problem of interface discretization, a major difficulty stems from the large size of the dam as compared to the process zone size. In fact, we have two distinct length scales: one is related to the dam size, the so-called structural or macroscopic size, and the other is a microscopic length scale related to the size of the process zone in front of the crack tip. To correctly capture

the progress of crack propagation, the size of the smallest finite element should be comparable with the process zone size. To obtain an accurate solution without refining the mesh for the continuum, we adopt the *virtual node technique* originally proposed by Zavarise et al. [34] and then applied to interface mechanical problems in [33]. The basic idea of this method consists in changing the integration scheme usually adopted in node-to-segment contact elements. The cohesive/contact contribution to the stiffness matrix and the internal force vector are in fact integrated on the contact element through a n -point Gauss integration scheme instead of a simpler 2-point Newton–Cotes integration formula. In this way, an arbitrary number of Gauss points can be specified inside each contact element along the interface, regardless of the discretization used for the continuum.

Moreover, another difficulty regards the use of cohesive zone models in dynamics. This often leads to rate-dependent numerical results, although the description of the material behavior does not explicitly include rate-dependent parameters (see [35] for a wide discussion on this topic). Numerical rate effects are due to the interplay between characteristic scales (length and time) of cohesive models and inertia. In particular, a very high loading rate seems to increase the peak stresses σ_{\max} and τ_{\max} and the fracture energy of the cohesive zone model with respect to a quasi-static analysis. This can be accounted for in the model by including a loading rate-dependency in the cohesive zone model, as proposed in [35]. However, this effect is not considered here for two reasons: there is a lack of experimental information about the dynamic behavior of real rock–concrete interfaces and the use of the same cohesive parameters as for the quasi-static case is in favor of safety. In any case, two characteristic time scales should be considered:

$$t_1 = \frac{\rho c_L l_{Nc}}{2\sigma_{\max}}, \quad t_2 = \frac{a_0}{c_L}, \quad (11)$$

where $c_L = \sqrt{E/\rho}$ is the dilatational wave speed of the material, computed as the square root of the ratio between the Young's modulus and the mass density, and a_0 is the length of the interface in front to the crack tip. Therefore, t_1 is the intrinsic time of the cohesive zone model operating in dynamics and therefore it is proportional to the time requested by a dilatational wave to cross the process zone. The other time, t_2 , comes from the fact we are analyzing a structural problem with finite boundaries in dynamics and it corresponds to the time necessary for a wave to travel along the whole bonded interface and reach the boundary of the dam, where it will be subjected to reflection.

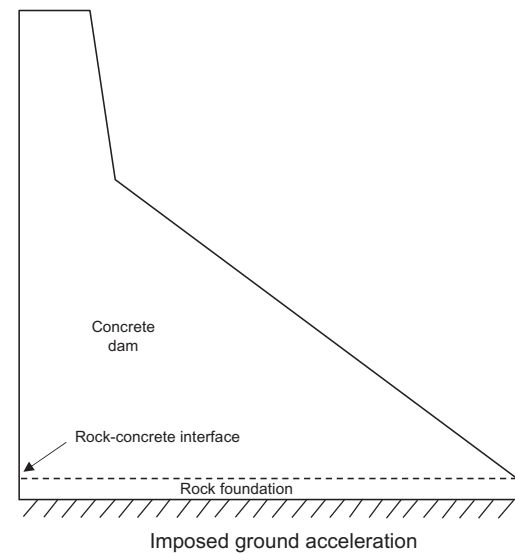
To deal with this two very different time scales, time integration is performed by using the Newmark formulae, explicit in the displacements and implicit in the velocities. The seismic action has been modeled giving the dam the same stiffness of the soil of foundation and with reference to P waves, neglecting S waves. The P waves (primary waves) are longitudinal compressional waves traveling along the interface faster than any other type of wave generated during an earthquake. A typical speed in rocks is 5000 m/s. The S waves (secondary waves) are shear waves transverse to the interface and induce displacements of the ground perpendicular to the direction of propagation. Obviously these hypotheses are a simplification of a real earthquake [36], which will be examined in a future paper.

5. Numerical example

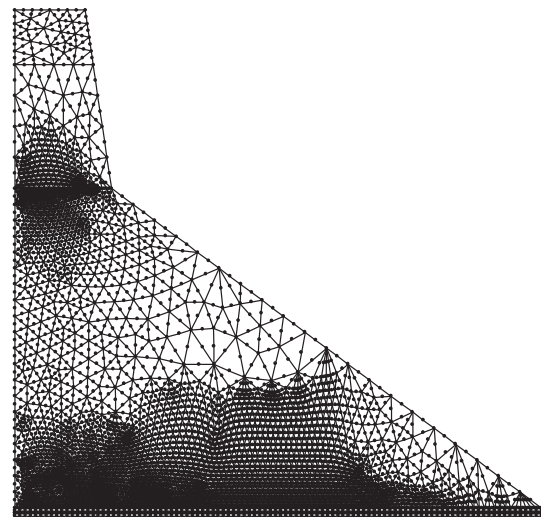
In this section, a numerical application of the proposed numerical model is presented for the analysis of separation at the cold interface between rock and concrete under the action of seismic loading. In order to analyze the effects of a real earthquake, we focus our attention on the Koyna dam geometry, for which the

ground accelerations were recorded and are used as input for the dynamic problem (see Fig. 8 for the geometry and the undeformed mesh of the dam). The dam height is 103 m, the crest width is 14.8 m, and the foundation width is 70 m. The reservoir height and width to assess the effect of fluid pressure are, respectively, 92 m and 300 m.

Plane strain triangular elements with linear shape functions are used for the discretization of the continuum. Regarding the rock–concrete interface at the foundation, the node-to-segment contact strategy is adopted, which does not require matching of nodes for the continuum elements sharing the interface. A very fine mesh is necessary to resolve the process zone tractions at the crack tip, as shown in Fig. 8(b). Regarding the material properties, a Young's modulus and a Poisson's ratio $E = 50$ GPa and $\nu = 0.2$ for both concrete and rock are considered. The mass density ρ of concrete and rock are chosen equal to 2500 kg/m³ and 2800 kg/m³, respectively. The parameters of the cohesive zone model are the same as those



(a) Sketch of the dam



(b) Undeformed mesh of the Koyna dam

Fig. 8. (a) Sketch of the Koyna dam with the position of the rock–concrete interface and (b) FE mesh.

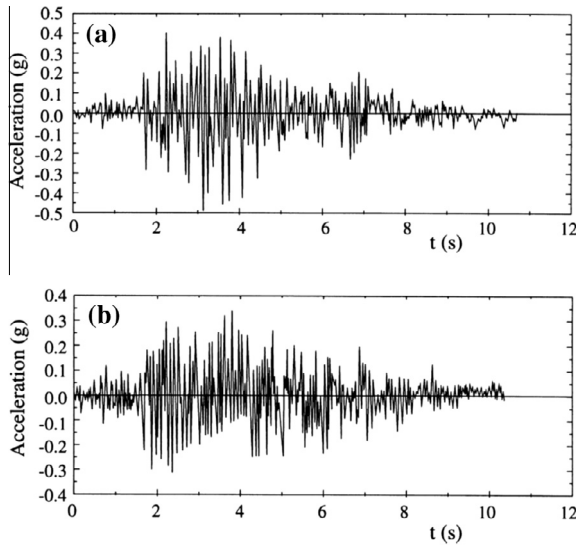


Fig. 9. Acceleration components in the horizontal (a) and vertical (b) directions used in the FE analysis [14].

used in Section 3. In particular, the peak stress of the CZM is set equal to the tensile strength of concrete, $\sigma_{max} = \sigma_u$, and the Mode I interface fracture energy as the fracture energy of concrete, $\mathcal{G}_{int} = \mathcal{G}_F$. Those values, used for the first step of the simulations, are consistent with those of large specimens, i.e., $\mathcal{G}_{int} = 250 \text{ N/m}$ and $\sigma_{max} = \tau_{max} = 3 \text{ MPa}$ (recent experimental results suggest that σ_{max} and τ_{max} are similar to each other [37]). For the friction coefficient, which may range from 0.6 to 0.3 depending on the size of the sample, we set $f = 0.3$ as a worst case scenario for a very large fault. All these input parameters are updated at each step of the

numerical simulations, according to the scaling laws presented in Section 2. In this context, the size of the sample b is the length of the interface already to fail. In absence of information regarding the evolution of damage in case of repeated loading, the damage parameter α is considered as a free variable and a parametric analysis is performed by selecting $\alpha = 1$ and $\alpha = 2$. On the other hand, we set $\beta = 0$.

The duration of the simulated earthquake is nearly 9 s, with acceleration peaks up to 0.4 g (see Fig. 9 and [14]). In addition to the dynamic excitation, the hydrostatic pressure and the dead load are considered in the simulation. Regarding the dynamic solution, a Rayleigh damping model is considered as in [7], with the damping matrix linearly expressed in terms of the mass and stiffness matrices. The Newmark parameters were also chosen as in [7] and we adopt a time step of 2.0 ms.

Typical horizontal and vertical displacements at the crest of the dam obtained during the simulations are shown in Fig. 10. These global displacements do not significantly depend on the value of α and are similar to those found in [7] according to LFM. As expected, horizontal displacements are much higher in modulus than the vertical ones, confirming that modeling Mode Mixity is an important issue for these problems. Moreover, note that the vertical displacements are often negative valued, implying a contact condition at the interface.

The evolution of damage along the interface strongly depends on α . The damage evolution along the rock–concrete interface in the case of $\alpha = 2$ is shown in Fig. 11(a) for different time steps (x denotes the horizontal distance from the upstream of the dam, where crack nucleates). The damage variable D is an increasing function of time and reaches unity for $t = 6.0 \text{ s}$. Afterwards, no tractions are transmitted along the nucleated real crack, whose final length reaches 1.1 m at $t = 6.3 \text{ s}$. (see also the deformed mesh in Fig. 12, along with the superimposed contour plot of the equivalent

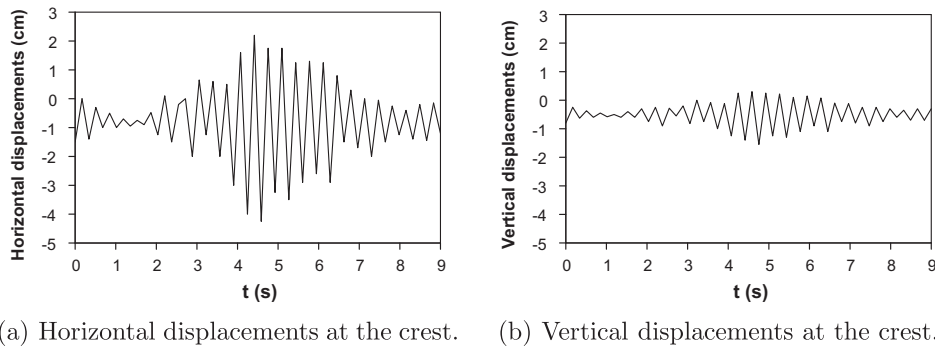


Fig. 10. Horizontal and vertical displacements at the crest of the dam vs. time.

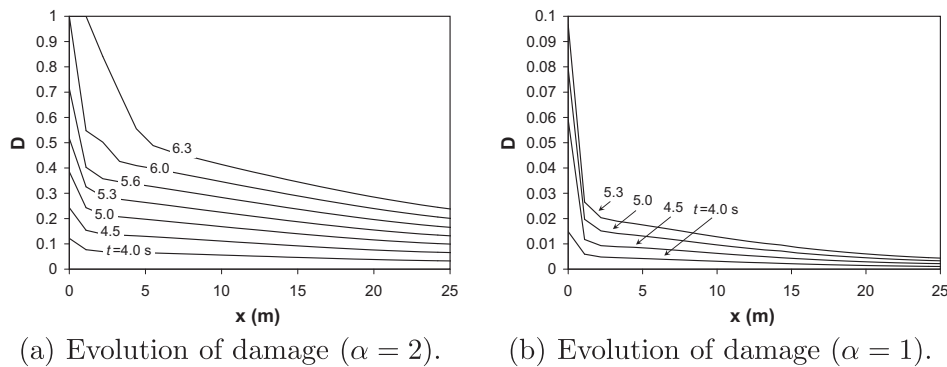


Fig. 11. Evolution of damage along the interface vs. time.

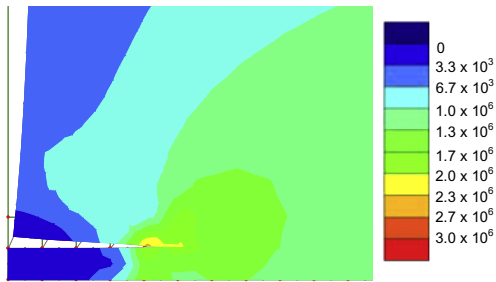


Fig. 12. Detail of the deformed mesh near the dam foundation (magnification factor = 400) and contour plot of von Mises stresses (Pa).

von Mises stresses). This detail represents the initial part of the rock–concrete interface in Fig. 8(a) on the reservoir side. On the other hand, when $\alpha = 1$, damage is much lower, being always less than 0.1 (see Fig. 11(b)).

6. Conclusion

Structural integrity assessment of concrete gravity dams has long been the subject of research. So far, most of the proposed numerical models based either on linear elastic (LEFM) or nonlinear fracture mechanics (NLFM) concerned the simulation of Mixed-Mode crack propagation under quasi-static loading, i.e., hydraulic and weight loads. Dam failure is often the result of crack propagation along concrete–concrete cold joints and along the rock–concrete interface at the dam foundation. Seismic fracture analyses are quite scarce due to their complexity, given the very different time scales and size scales to be dealt with. Moreover, cracks in dams require special modeling when subjected to repeated loadings, as it happens during an earthquake. This requires a proper modeling of fracture, using NLFM, of crack closure, satisfying the unilateral contact condition, and of damage evolution.

The selection of suitable interface fracture and contact parameters is particularly relevant. The examination of the literature on cold interfaces suggests that the results regarding the size-scale effects on tensile strength and fracture energy of concrete can also be used to characterize the behavior of the interface, at least up to a certain extent. Further experimental results are indeed required to characterize the behavior of cold interfaces under repeated loading, an issue that has not yet been investigated with required accuracy.

In the present study, the unified interface constitutive law proposed in [17] for modeling quasi-static fracture in fiber reinforced composites has been applied to the analysis of interface dynamic crack propagation in concrete gravity dams. The numerical simulation in Section 5 has been proposed with the aim to show the capability of the proposed modeling strategy based on the integration of the cohesive zone model, micromechanically-based contact formulations and damage mechanics. For the sake of simplicity, the case of an interface crack at the foundation has been analyzed, since it is often considered very dangerous and difficult to be inspected. Numerically, the direction of crack propagation was known a priori, simplifying the computations. Other locations of crack propagation are also possible and cannot be excluded. In the most general case, a crack could propagate under Mode Mixity inside the concrete blocks. This scenario, however, requires the determination of the direction of crack propagation, which is no longer defined by the interface line, and a suitable meshing algorithm to adaptively insert either interface or contact elements. For this complexity, this investigation is left for further research, where the interplay between different nonlinear cracks in dynamics will be rigorously analyzed.

Although further investigations are certainly required to better define the range of variability of the parameters entering the damage model, the application to the Koyna dam shows that it is possible to simulate interface crack propagation and that the exponent α has an important effect on the evolution of damage.

References

- [1] Pal W. Seismic cracking of concrete gravity dam. *J Struct Div ASCE* 1976;102(ST9):1827–44.
- [2] Linsbauer HN. Fracture mechanics models for characterizing crack behaviour of gravity dams. In: *Proceedings of the 15th ICOLD*, Lausanne 1985;2. p. 279–291.
- [3] Fanelli M, Giuseppetti G. Advanced dam analysis. *Eng Fract Mech* 1990;35:525–30.
- [4] Chappell JF, Ingraffea AR. A fracture mechanics investigation of the cracking of Fontana dam, Department of Structural Engineering, Report 81-7, Cornell University, Ithaca, New York; 1981.
- [5] Ingraffea AR. Case studies of simulation of fracture in concrete dams. *Eng Fract Mech* 1990;35:553–64.
- [6] Chapuis J, Rebora B, Zimmermann T. Numerical approach of crack propagation analysis in gravity dams during earthquakes. In: *Proceedings of the 15th ICOLD*, Lausanne, 1985;2. p. 451–473.
- [7] Ayari ML, Saouma VE. A fracture mechanics based seismic analysis of concrete gravity dams using discrete cracks. *Eng Fract Mech* 1990;35:587–98.
- [8] Jirásek M, Zimmermann T. Analysis of the rotating crack model. *J Eng Mech ASCE* 1998;124:842–51.
- [9] Lin, Shan-Wern S, Ingraffea AR. Case studies of cracking of concrete dams—a linear elastic approach, Department of Structural Engineering, Report 88-2, Cornell University, Ithaca, New York; 1988.
- [10] Linsbauer HN, Ingraffea AR, Rossmanith HP, Wawrzynek PA. Simulation of cracking in large arch dam: Part I. *J Struct Eng ASCE* 1989;115:1599–615.
- [11] Linsbauer HN, Ingraffea AR, Rossmanith HP, Wawrzynek PA. Simulation of cracking in large arch dam: Part II. *J Struct Eng ASCE* 1989;115:1616–30.
- [12] Bažant ZP, Le J-L, Bažant MZ. Scaling of strength and lifetime probability distributions of quasibrittle structures based on atomistic fracture mechanics. *Proc Nat Acad Sci USA* 2009;106:11,484–11489.
- [13] Carpinteri A, Valente S, Ferrara G, Imperato L. Experimental and numerical fracture modelling of a gravity dam. In: Bažant ZP, editor. *Fracture Mechanics of Concrete Structures*. The Netherlands: Elsevier; 1992. p. 351–60.
- [14] Guanglun W, Pekau OA, Chuhan Z, Shaomin W. Seismic fracture analysis of concrete gravity dams based on nonlinear fracture mechanics. *Eng Fract Mech* 2000;65:67–87.
- [15] Barpi F, Valente S. Numerical simulation of prenotched gravity dam models. *J Eng Mech ASCE* 2000;126:611–29.
- [16] Paggi M, Ferro G, Braga F. Seismic analysis of concrete gravity dams: nonlinear fracture mechanics models and size-scale effects. *Appl Mech Mater* 2011;82:374–9.
- [17] Paggi M, Carpinteri A, Zavarise G. A unified interface constitutive law for the study of fracture and contact problems in heterogeneous materials. In: Wriggers P, Nackenhorst U, editors. *Analysis and Simulation of Contact Problems*. Lecture Notes in Applied and Computational Mechanics, vol. 27. Berlin: Springer-Verlag; 2006. p. 297–304.
- [18] Ghaemmaghami A, Ghaemian M. Large-scale testing on specific fracture energy determination of dam concrete. *Int J Fract* 2006;141:47–254.
- [19] Carpinteri A. Scaling laws and renormalization groups for strength and toughness of disordered materials. *Int J Solids Struct* 1994;31:291–302.
- [20] Carpinteri A, Ferro G. Size effects on tensile fracture properties: a unified explanation based on disorder and fractality of concrete microstructure. *Mater Struct* 1994;27:563–71.
- [21] Carpinteri A, Chiaia B. Multifractal nature of concrete fracture surfaces and size effects on nominal fracture energy. *Mater Struct* 1995;28:435–43.
- [22] Ferro G. On dissipated energy density in compression for concrete. *Eng Fract Mech* 2006;73:1510–30.
- [23] Chandra Kishen JM, Subba Rao P. Fracture of cold jointed concrete interfaces. *Eng Fract Mech* 2007;74:122–31.
- [24] Carpinteri A, Paggi M. Size-scale effects on strength, friction and fracture energy of faults: a unified interpretation according to fractal geometry. *Rock Mech Rock Eng* 2008;41:735–46.
- [25] Bandis S, Lumsden AC, Barton NR. Experimental studies of scale effects on the shear behaviour of rock joints. *Int J Rock Mech Min Sci Geomech Abstr* 1981;18:1–21.
- [26] Geubelle PH, Baylor JS. Impact-induced delamination of composites: a 2D simulation. *Compos Part B: Eng*. 1998;29:589–602.
- [27] Kubair DV, Geubelle PH. Comparative analysis of extrinsic and intrinsic cohesive models of dynamic fracture. *Int J Solids Struct* 2003;40:3853–68.
- [28] Panagiotopoulos PD. *Inequality problems in mechanics and applications*. Basel: Birkhäuser Verlag; 1985.
- [29] Paggi M, Barber JR. Contact conductance of rough surfaces composed of modified RMD patches. *Int J Heat Mass Transf* 2011;4:4664–72.
- [30] Wriggers P. *Computational contact mechanics*. England: John Wiley & Sons, Ltd.; 2002.
- [31] Roe KL, Siegmund T. An irreversible cohesive zone model for interface fatigue crack growth simulations. *Eng Fract Mech* 2003;70:209–32.

- [32] Paggi M. Modelling fatigue in quasi-brittle materials with incomplete self-similarity concepts. *RILEM Mat Struct* 2011;44:659–70.
- [33] Carpinteri A, Paggi M, Zavarise G. The effect of contact on the decohesion of laminated beams with multiple microcracks. *Int J Solids Struct* 2008;45:129–43.
- [34] Zavarise G, Boso D, Schrefler B. A contact formulation for electrical and mechanical resistance. In: *Proceedings of CMIS, III Contact Mechanics International Symposium, Praja de Consolacao, Portugal; 2001*. p. 211–218.
- [35] Corigliano A, Mariani S, Pandolfi A. Numerical analysis of rate-dependent dynamic composite delamination. *Compos Sci Tech* 2006;66:766–75.
- [36] Masi A, Chiauzzi L, Braga F, Mucciarelli M, Vona M, Ditommaso R. Peak and integral seismic parameters of l'Aquila 2009 ground motions: observed versus code provision values. *Bull Earthquake Eng* 2011;9:139–56.
- [37] Fishman Yu A. Stability of concrete retaining structures and their interface with rock foundations. *Int J Rock Mech Min Sci* 2009;46:957–66.